

Thermophysical analysis for three-dimensional MHD stagnation-point flow of nano-material influenced by an exponential stretching surface

Fiaz Ur Rehman^{a,*}, Sohail Nadeem^b, Hafeez Ur Rehman^c, Rizwan Ul Haq^d

^a Department of Mathematics, Govt. Postgraduate College No. 1, Abbottabad 22010, Pakistan

^b Department of Mathematics, Quaid-I-Azam University, Islamabad 44000, Pakistan

^c Department of Computer Science, National University of Computer and Emerging Sciences, Peshawar, Pakistan

^d Department of Electrical Engineering, Bahria University, Islamabad Campus, Islamabad 44000, Pakistan



ARTICLE INFO

Article history:

Received 12 October 2017

Received in revised form 10 December 2017

Accepted 11 December 2017

Available online 16 December 2017

Keywords:

Heat transfer

Nanofluids

Stagnation-point flow

Three-dimensional flow

Nano particles

Boundary layer

ABSTRACT

In the present paper a theoretical investigation is performed to analyze heat and mass transport enhancement of water-based nanofluid for three dimensional (3D) MHD stagnation-point flow caused by an exponentially stretched surface. Water is considered as a base fluid. There are three (3) types of nanoparticles considered in this study namely, CuO (Copper oxide), Fe_3O_4 (Magnetite), and Al_2O_3 (Alumina) are considered along with water. In this problem we invoked the boundary layer phenomena and suitable similarity transformation, as a result our three dimensional non-linear equations of describing current problem are transmuted into nonlinear and non-homogeneous differential equations involving ordinary derivatives. We solved the final equations by applying homotopy analysis technique. Influential outcomes of aggressing parameters involved in this study, effecting profiles of temperature field and velocity are explained in detail. Graphical results of involved parameters appearing in considered nanofluid are presented separately. It is worth mentioning that Skin-friction along x and y -direction is maximum for Copper oxide-water nanofluid and minimum for Alumina-water nanofluid. Result for local Nusselt number is maximum for Copper oxide-water nanofluid and is minimum for magnetite-water nanofluid.

© 2017 The Authors. Published by Elsevier B.V. This is an open access article under the CC BY-NC-ND license (<http://creativecommons.org/licenses/by-nc-nd/4.0/>).

Introduction

The in depth study of flow phenomena focusing on stagnation-point flows and stretching surface is vital in the field of fluid mechanics and it has gained concentration of researchers after its useful practical applications in the industry, like flows observed over the tip of aircrafts and submarines. The spinning, floating and blowing of fiber glass is one of the best examples where flow caused by stretching plate near stagnation point can be detected. Hiemenz [1] was the leading researcher who investigated steady 2-D stagnation point flow and found its exact solution. Similarly, Howath [2] studied the flow near time-independent axisymmetric stagnation point. After that many researchers are involved in the study of flows involving stagnation point phenomena, like Chiam [3], Mahapatra and Gupta [4,5], Nazar et al. [6], Reza and Gupta [7], Lok et al. [8,9], etc. The researchers investigated the problem of boundary layers flow with heat transport effects when a sheet is stretched. Chiam [3] reported the 2-D stagnation-point flow in combination with stretching sheet problem and he revealed the

interesting outcome that flow profile closer to stretching surface shows similar behavior as inviscid flow which is far away from surface yielding a nowhere boundary layer flow. Mahapatra and Gupta [5] illustrated contrary to the outcomes of Chiam [3]. There are a notable number of papers in the literature in which flow describing stagnation-point phenomena owing to a stretching sheet/surface is center of the study. Some of them include Ul Haq et al. [10], Rosali et al. [11], Mabood et al. [12], Hsiao [13] and Ur Rehman et al. [14], among others.

Enhancement of heat transfer by using nanofluids have attracted a lot of researcher because of their applications in fields like biocatalysis, bio-labeling, biosensors, purification and separation of biomolecules, transportation (Cooling of engine/thermal management of vehicle), cooling in nuclear systems, thermal storage, solar water heating, material manufactured by aerodynamic excursion and polymer excursion, glass fiber production, space, defense, magnetic resonance imaging (MRI), drug delivery, thermal absorption system etc. Choi [15] was the first researcher who used the word “nanofluids” at the ASME Winter Annual Meeting in 1995. From the appraisal of thermal assets it is a major problem with conventional heat transport liquids like bio-fluids, ethylene glycol, water, oil and lubricants that they lack in greater heat trans-

* Corresponding author.

E-mail address: tanolig@gmail.com (F. Ur Rehman).

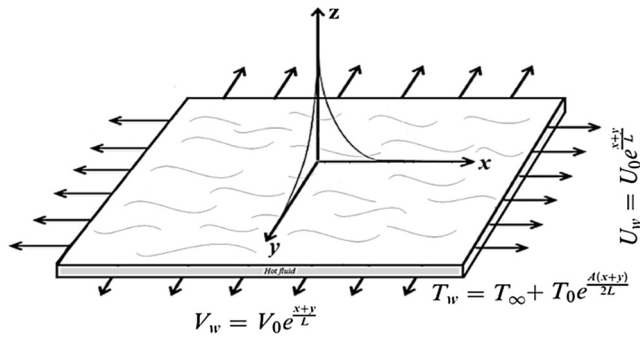


Fig. 1. Geometrical configuration of flow problem.

tively. After applying above suppositions the governing equation [34] can be represented in usual notations as:

$$u_x + v_y + w_z = 0, \tag{1}$$

$$uu_x + vv_y + ww_z = -\frac{1}{\rho_{nf}} p_x + \nu_{nf} \left(u_{zz} - \frac{\sigma^* B_0^2}{\rho} u \right), \tag{2}$$

$$uv_x + vv_y + ww_z = -\frac{1}{\rho_{nf}} p_y + \nu_{nf} \left(v_{zz} - \frac{\sigma^* B_0^2}{\rho} v \right), \tag{3}$$

$$uT_x + vT_y + wT_z = \alpha_{nf} T_{zz}, \tag{4}$$

Associated boundary conditions are

$$z = 0, u = U_w, v = V_w, w = 0, T = T_w, \tag{5}$$

$$z \rightarrow \infty, u = U_s(x, y), v = V_s(x, y), w = 0, T = T_\infty. \tag{6}$$

Here subscript ‘w’ refers the condition on wall. In this study we assumed that the surface stretching velocities, wall temperature and free stream velocity are

$$U_w(x, y) = U_0 e^{\frac{(x+y)}{L}}, V_w(x, y) = V_0 e^{\frac{(x+y)}{L}}, T_w(x, y) = T_\infty + T_0 e^{\frac{A(x+y)}{2L}}, \tag{7}$$

$$U_s(x, y) = U_e e^{\frac{(x+y)}{L}}, V_s(x, y) = V_e e^{\frac{(x+y)}{L}}, \tag{8}$$

where T_0, U_0, V_0, U_e and V_e are all constants, U_s and V_s are free stream velocities, T_∞ is ambient fluid temperature, L specifies reference length, and A intends the temperature exponent. The effective density ρ_{nf} and the effective viscosity μ_{nf} given by Brinkman [52], are expressed as

$$\mu_{nf} = \frac{\mu_f}{(1 - \phi)^{2.5}}, \quad \rho_{nf} = \phi \rho_s + (1 - \phi) \rho_f, \tag{9}$$

The heat capacitance $(\rho C_p)_{nf}$ and thermal diffusivity α_{nf} of nanofluid as given by Xuan and Li [53] are defined as

$$(\rho C_p)_{nf} = \phi (\rho C_p)_s + (\rho C_p)_f (1 - \phi), \quad \alpha_{nf} = \frac{k_{nf}}{(\rho C_p)_{nf}}, \tag{10}$$

The effective thermal conductivity k_{nf} and viscosity ν_{nf} are obtained experimentally [54] and are given by

$$\frac{k_{nf}}{k_f} = \frac{(k_s + 2k_f) - 2\phi(k_f - k_s)}{(k_s + 2k_f) + \phi(k_f - k_s)}, \quad \nu_{nf} = \frac{\mu_{nf}}{\rho_{nf}}, \tag{11}$$

A similarity transformation [23] is introduced as

$$u = U_e e^{\frac{(x+y)}{L}} f'(\eta), v = U_e e^{\frac{(x+y)}{L}} g'(\eta), w = -\left(\frac{\nu U_e}{2L}\right)^{1/2} e^{\frac{(x+y)}{2L}} [f + \eta f' + g + \eta g'],$$

$$T = T_\infty + T_0 e^{\frac{A(x+y)}{2L}} \theta(\eta), \eta = \left(\frac{U_e}{2\nu L}\right)^{1/2} e^{\frac{(x+y)}{2L}} z, \tag{12}$$

and our basic Eqs. (2)–(4) are transmuted into following three ordinary differential equations (ODEs):

$$\frac{1}{(1 - \phi + \phi(\rho_s/\rho_f))(1 - \phi)^{2.5}} f'''' = -f''(f + g) + 2f'(f' + g') + M(f' - 1) - 2(1 + r_1), \tag{13}$$

$$\frac{1}{(1 - \phi + \phi(\rho_s/\rho_f))(1 - \phi)^{2.5}} g'''' = -g''(f + g) + 2g'(f' + g') + Mr_1(g' - 1) - 2(1 + r_1)r_1, \tag{14}$$

$$\frac{1}{Pr} \left[\frac{k_{nf}/k_f}{(1 - \phi) + \phi((\rho C_p)_s/(\rho C_p)_f)} \right] \theta'' = -(f + g)\theta' + A(f' + g')\theta, \tag{15}$$

Now corresponding boundary conditions (5) and (6) become

$$f(0) = 0 = g(0), f'(0) = \alpha_1, g'(0) = \alpha_2, \theta(0) = 1, \tag{16}$$

$$f'(\infty) = 1, g'(\infty) = r_1, \theta(\infty) = 0. \tag{17}$$

Here the primes stand for differentiation of function with respect to η , $\alpha_1 = U_0/U_e$ and $\alpha_2 = V_0/U_e$ represent wall stretching ratios, $r_1 = V_e/U_e$ is stagnation point, $M = \frac{\sigma B_0^2}{\rho U_s}$ is the Hartmann number and $Pr = (\mu C_p)_f/k_f$ is referred as the Prandtl number. The first two terms in Eq. (16) arise from the no-penetration wall condition, $f(0) + g(0) = 0$. Without loss of generality, Eq. (16) is used instead. Note that the continuity Eq. (1) has been satisfied by assuming the form defined in Eq. (12). Eqs. (13)–(17) demonstrate that the non-homogeneous hydrodynamic problem contains three parameters in the boundary conditions, on the other hand heat transport problem contains two additional parameters in the equation.

The physical properties of much importance are the dimensionless coefficients of surface skin-friction c_{fx} and c_{fy} , along both directions, and the local Nusselt number defined as

$$c_{fx} = \frac{\tau_{wx}}{\rho_f U_0^2/2}, \quad c_{fy} = \frac{\tau_{wy}}{\rho_f U_0^2/2}, \quad Nu_x = \frac{xq_w}{k_f(T - T_\infty)}, \tag{18}$$

where τ_{wx} and τ_{wy} are shear stresses in the x - and y -directions, respectively, and q_w represents heat flux of surface. These are defined as

$$\tau_{wx} = \mu_{nf}(u_z + w_x)_{z=0}, \tau_{wy} = \mu_{nf}(v_z + w_y)_{z=0}, q_w = -k_{nf}T_z|_{z=0}, \tag{19}$$

Using Eqs. (12) and (19), we get

$$Re_x^{1/2} C_{fx}/2e^{\frac{3(x+y)}{2L}} = \frac{1}{(1 - \phi)^{2.5}} f''(0), \tag{20}$$

$$Re_y^{1/2} C_{fy}/2e^{\frac{3(x+y)}{2L}} = \frac{1}{(1 - \phi)^{2.5}} g''(0), \tag{21}$$

$$Re_x^{-1/2} Nu_x/2e^{\frac{x+y}{2L}} \frac{x}{L} = -\frac{k_{nf}}{k_f} \theta'(0), \tag{22}$$

where Re symbolizes Reynolds number defined as $Re = U_0 L/\nu$.

Solution technique

To obtain the solutions of Eqs. (13)–(15), we adopted frequently used Homotopy analysis technique (HAM) [54–58]. It is a powerful analytic type technique for solving non-linear, ordinary as well as partial differential equations. In 1992, Liao developed this analytical technique. This technique can be used to solve weak as well as

strongly non-linear mathematical models due to the fact that it does not depend on small physical parameter confinement. While using this technique we can adapt the convergence of solution using base functions and supplementary parameters. In the present study our initial guesses and their corresponding operators are listed below

$$\left. \begin{aligned} f_0(\eta) &= \eta + (\alpha_1 - 1) * (1 - \exp(-\eta)), \\ g_0(\eta) &= (\alpha_2 - r_1) + r_1 * \eta + (r_1 - \alpha_2) * (1 - \exp(-\eta)), \\ \theta_0(\eta) &= \exp(-2\eta). \end{aligned} \right\} \quad (23)$$

$$\mathcal{L}_f = \frac{d^3 f}{d\eta^3} - \frac{df}{d\eta}, \quad \mathcal{L}_g = \frac{d^3 g}{d\eta^3} - \frac{dg}{d\eta}, \quad \mathcal{L}_\theta = \frac{d^2 \theta}{d\eta^2} - 4\theta, \quad (24)$$

Convergence analysis

The rapid convergence of generated solution after employing Homotopy analysis technique greatly relies on the best selection of supplementary parameter h_f, h_g, h_θ . The usefulness of obtained solution highly depends on the rate of convergence. Hence we have diagrammed h -curves for CuO-water in Fig. 2 in order to obtain the legitimate values of h_f, h_g and h_θ .

After going through Fig. 2 we observe that the permissible range for auxiliary parameters is $-1.3 \leq h_f, h_g \leq -0.3, -1.7 \leq h_\theta \leq -0.2$. It is observed that the series solution will be convergent in the whole realm of $\eta(0 < \eta < \infty)$ by selecting $h_f = h_g = h_\theta = -0.75$. After investigation of outcomes in above table, it is guaranteed that the desired convergence is attained at 30th order.

Final outcomes and discourse of results

In the present section we shall thoroughly explain the behavior of important parameters on dimensionless velocities, temperature, skin frictions and heat transport for (water-based) nanofluid. The egressing parameters are nanoparticle volume fraction ϕ , stretching parameters α_1 and α_2 , stagnation point parameter r_1 , Hertmann number M , and temperature exponent parameter A as shown in Figs. 3–16 for water-based nanofluids. There are three characters of nanoparticles under consideration in the present study namely, CuO (Copper oxide), Fe_3O_4 (Magnetite), and Al_2O_3 (Alumina). These three nanoparticles were also considered by different researcher [21,23,30,31,59] for different heat transport problems. In the investigation conducted by Oztop and Abu-Nada [59], they selected $Pr = 6.2$ (for water) and ϕ is taken as $0 \leq \phi \leq 0.2$ where $\phi = 0$ refers the Newtonian type fluid. Also we have listed thermophysi-

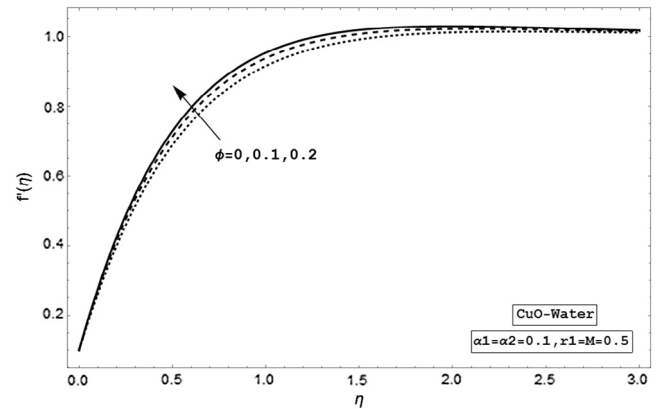


Fig. 3. Variation of ϕ influencing velocity profile $f'(\eta)$.

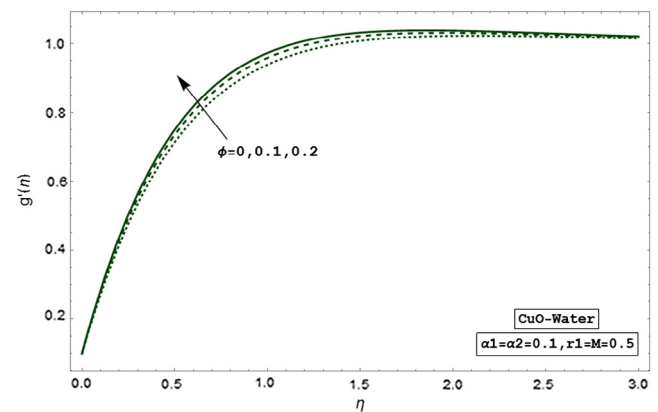


Fig. 4. Variation of ϕ influencing velocity profile $g'(\eta)$.

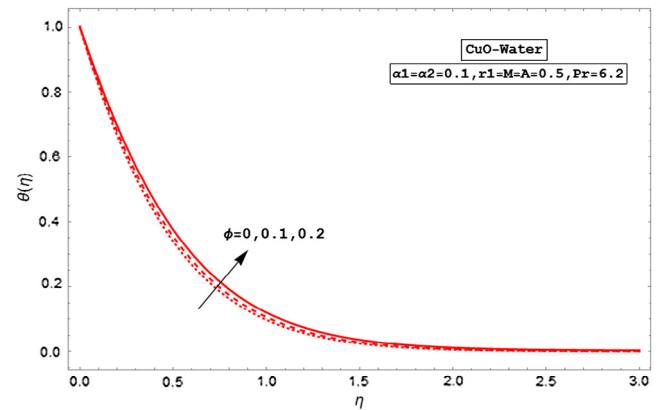


Fig. 5. Variation of ϕ influencing temperature profile $\theta(\eta)$.

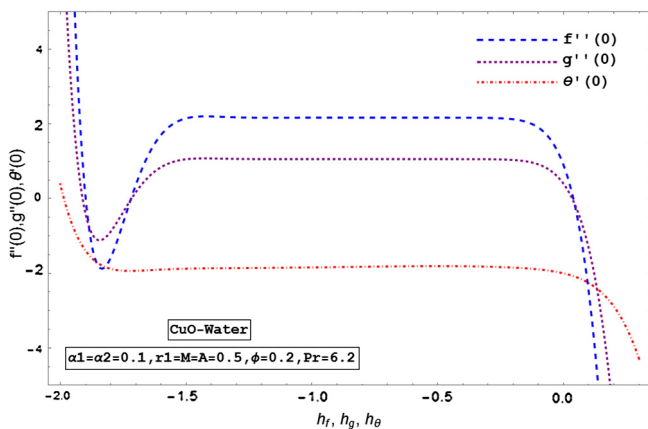


Fig. 2. h - curves for the functions $f(\eta), g(\eta)$ and $\theta(\eta)$.

cal characteristics of chosen base fluid (water) and three different nanoparticles (1–100 nm) in Table 2.

From graphical results we observed that in presence of magnetic effects and stagnation point flow all velocities $f'(\eta)$ and $g'(\eta)$ start from their wall values α_1 and α_2 respectively. As η increases, $f'(\eta)$ approaches 1 and $g'(\eta)$ approaches the stagnation point r_1 . The temperature profile $\theta'(\eta)$ decreases from unity (1) to zero (0) as dimensionless distance η grows from starting position zero to infinity. This section contains Figs. 3–16. These Figures are exhibited in order to see the exciting results of several parameters which effect velocity and temperature behavior. Figs. 3–5

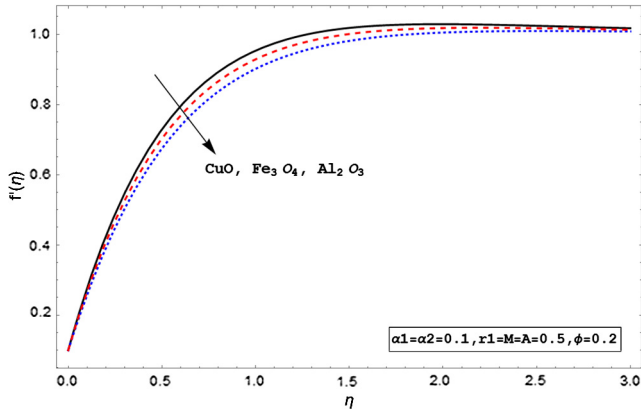


Fig. 6. Influence of nanoparticles on velocity profile $f'(\eta)$.

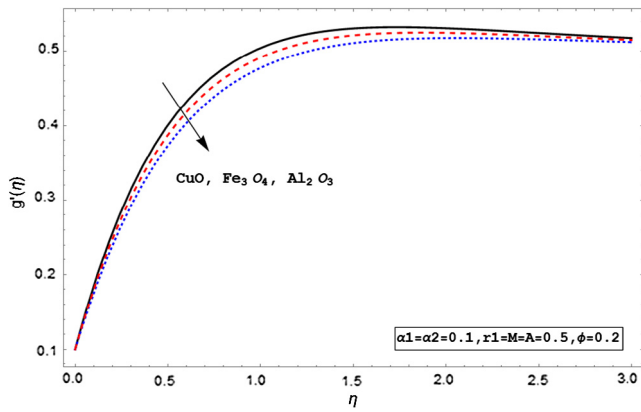


Fig. 7. Influence of nanoparticles on velocity profile $g'(\eta)$.

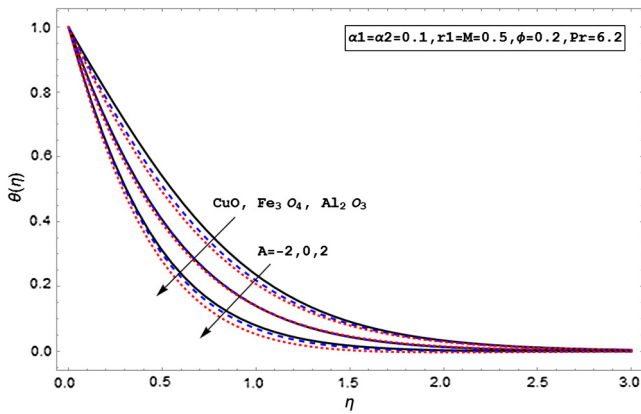


Fig. 8. Influence of nanoparticles on temperature profile $\theta(\eta)$.

illustrates the consequences of CuO-nanoparticle volume fraction ϕ and stagnation point r_1 on the dimensionless velocity as well as temperature profiles. It is observed that an enhancement in ϕ tends to a growing behavior in the dimensionless velocities and temperature. As stagnation point $r_1 (\geq \alpha_2)$ increases, the dimensionless velocities show an increase whereas temperature profile tends to decrease.

Figs. 6–8 elucidate the influence of different nanoparticles under consideration including Copper oxide (CuO), Magnetite (Fe₃O₄), and alumina (Al₂O₃) and they are effecting velocity, temperature profiles. From Figs. 6 and 7 we can easily analyze that

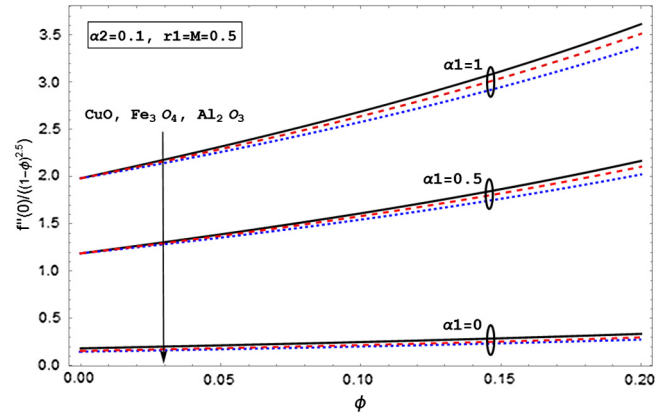


Fig. 9. Influence of ϕ and α_1 for different nanoparticles on skin friction coefficient along x -axis.

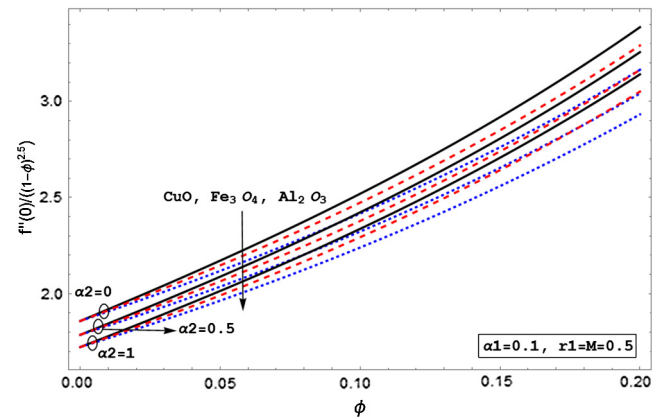


Fig. 10. Influence of ϕ and α_2 for different nanoparticles on skin friction coefficient along x -axis.

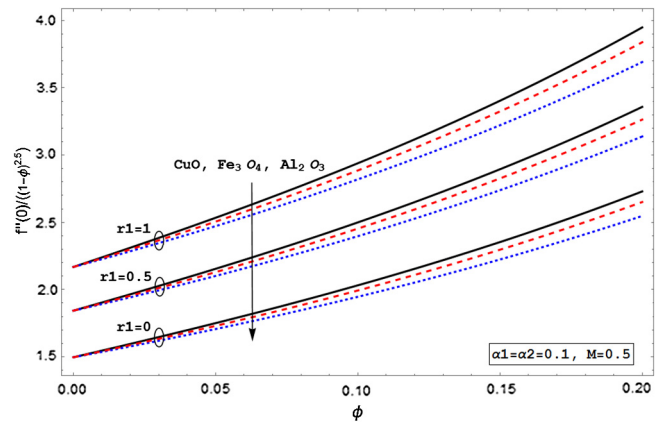


Fig. 11. Influence of ϕ and r_1 for different nanoparticles on skin friction coefficient along x -axis.

CuO–water nanofluid has maximum velocity in comparison with Fe₃O₄–water and Al₂O₃–water nanofluids in both directions.

It also explains the maximum velocity of Fe₃O₄–water nanofluid over Al₂O₃–water nanofluid. Fig. 8 explains the thermal boundary layer is thicker for Al₂O₃–water nanofluid as compared to the other two. Also by increasing the temperature exponent parameter A, we conclude enhancement in thickness of boundary layer (thermal) is noticed. In absence of magnetic field and taking $\alpha_2 = r_1 = 0$, we

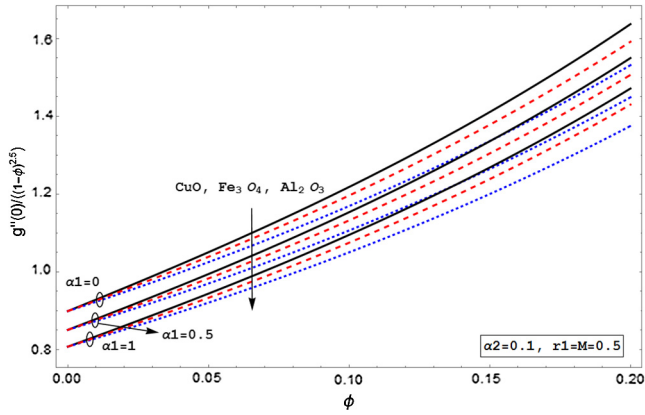


Fig. 12. Influence of ϕ and α_1 for different nanoparticles on skin friction coefficient along y-axis.

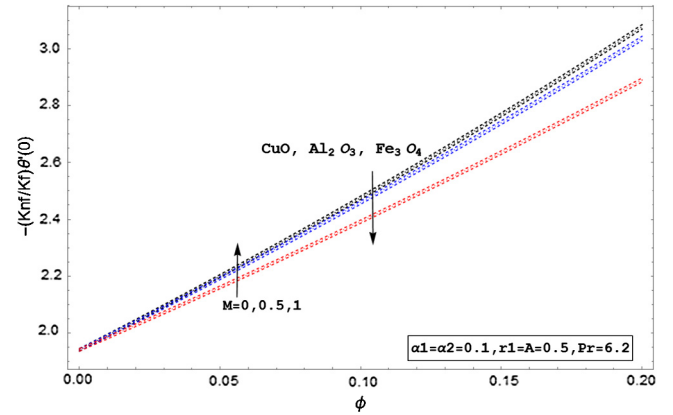


Fig. 15. Influence of ϕ and M for different nanoparticles on Nusselt number.

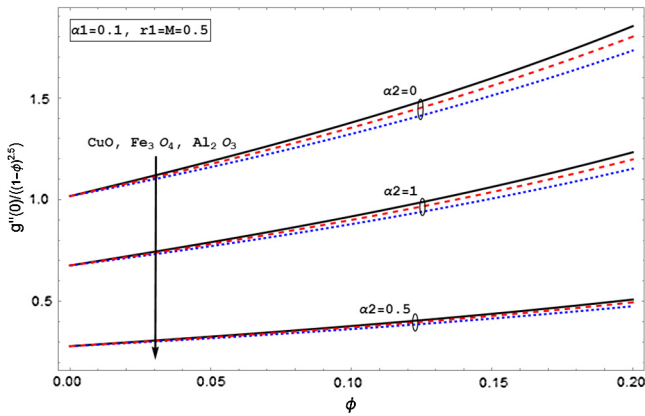


Fig. 13. Influence of ϕ and α_2 for different nanoparticles on skin friction coefficient along y-axis.

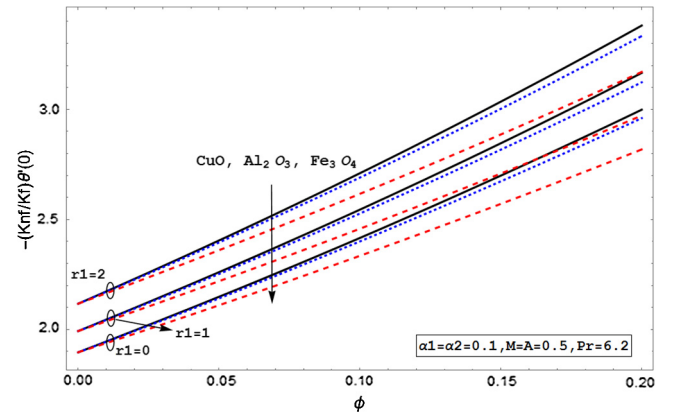


Fig. 16. Influence of ϕ and r_1 for different nanoparticles on Nusselt number.

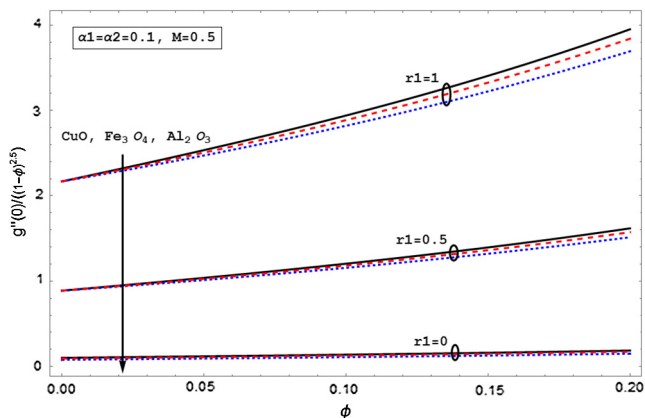


Fig. 14. Influence of ϕ and α_1 for different nanoparticles on skin friction coefficient along y-axis.

Table 1

Convergence of Homotopy solution for **CuO**-Water when $r_1 = 0.5, \alpha_1 = \alpha_2 = \phi = 0.1, Pr = 6.2, A = M = 0.5, h_f = h_g = h_0 = -0.75$.

Order of approximation	$-f''(0)$	$-g''(0)$	$-\theta'(0)$
1	1.747	0.834	1.925
10	2.171	1.060	1.805
20	2.169	1.061	1.835
30	2.169	1.061	1.859
40	2.169	1.061	1.859
50	2.169	1.061	1.859

compared the current study (Al_2O_3 -water nanofluid) with literature [44] in Table 3. Both results represented in Table 3 show a good agreement. Therefore we believe that present results are accurate.

Figs. 9–14 present the change in skin-friction with governing parameters α_1, α_2 and r_1 along x and y-direction respectively. In Figs. 9–11 it is depicted that the resistance to the flow in x increases for increasing α_1 and r_1 and falls for rising α_2 . It is important to note

that in each particular case along x-axis, the skin friction remained maximum for Copper Oxide-water nanofluid whereas minimum for Alumina-water nanofluid. On the other hand Figs. 12–14 explains that skin friction in y-direction increases for growing values of stagnation-point r_1 , and shows a decrease for growing values of stretching parameters α_1 . As α_2 varies, the skin friction in y-direction is maximum for $\alpha_2 = 0$ and minimum for $\alpha_2 = 0.5$. In Figs. 12–14 for each particular case along y-axis, the skin friction remained maximum for Copper Oxide-water nanofluid whereas it was minimum for Alumina-water nanofluid. The fluctuation of heat transport rate with the governing parameters is shown in Figs. 15–17. It is quite evident from Fig. 15 that as Hartmann number M increases, the heat transport rate also increases. Also for varying values of M , The maximum heat flux is reported for Copper oxide-water nanofluid and minimum for magnetite-water nanofluid. Similar behavior can be observed for heat flux against temperature exponent parameter A and stagnation point parameter r_1 in Figs. 16 and 17.

Table 2
Thermophysical properties of considered nanoparticles along water [30,31].

Physical Properties	Base-Fluid (water)	CuO	Al ₂ O ₃	Fe ₃ O ₄
C_p (J/kgK)	4179	531.8	765	670
k (W/mK)	0.613	76.5	40	9.7
ρ (kg/m ³)	997.1	6320	3970	36

Table 3
Comparison with the literature for stagnation-point flow of Al₂O₃-water nanofluid $r_1 = \alpha_2 = M = 0, Pr = 6.2, A = 1, h_f = h_g = h_0 = -0.75$.

α_1	ϕ	$\frac{1}{(1-\phi)^{2.5}} f''(0)$		$-\frac{k_{nf}}{k_f} \theta'(0)$	
		Bachok et al. [36]	Present results	Bachok et al. [36]	Present results
0	0	1.6872	1.6872	1.7148	1.7148
	0.1	2.1929	2.19293	2.0230	2.02301
	0.2	2.8174	2.81750	2.3345	2.33440
0.5	0	0.9604	0.96040	2.4874	2.48741
	0.1	1.2483	1.24829	2.8478	2.84784
	0.2	1.6039	1.60399	3.2235	3.22355

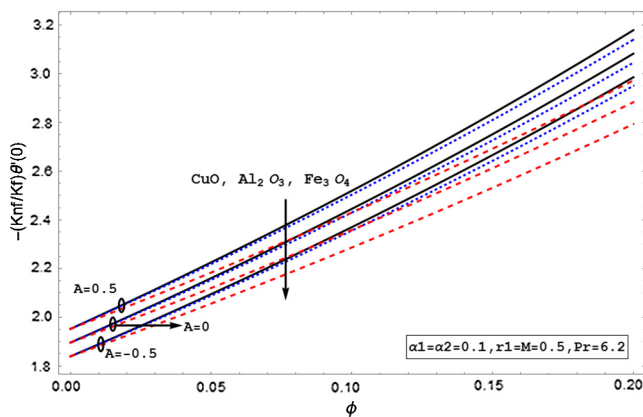


Fig. 17. Influence of ϕ and A for different nanoparticles on Nusselt number.

Concluding remarks

The whole investigation is reported for flow and heat transport enhancement for MHD 3-D stagnation-point flow of water-based nanofluid caused by a confined surface which is stretched exponentially. The suspended nanoparticles in current study were CuO (Copper oxide), Fe₃O₄ (Magnetite), and Al₂O₃ (Alumina). This study also assumes that the temperature specified at the surface varies exponentially. The developed mathematical model is tackled by homotopy analysis technique. We observed in current study that

- Nanoparticle volume fraction (symbolized as ϕ) appreciably enhances the dimensionless temperature and velocity field.
- Nanoparticle volume fraction also results in enhancement of skin friction and heat flux.
- The stagnation point parameter r_1 increases produced velocity and thermal profile whereas decreases induced boundary layer thickness in each case.
- Influence of temperature exponent (symbolized as A) is to increase temperature profile, thermal boundary layer and heat flux.
- From graphical results we can conclude that Skin-friction along x and y -direction is greater for CuO-water nanofluid and lesser for Al₂O₃-water nanofluid.

- The resulting quantity of local Nusselt number came out greater for CuO-water nanofluid whereas lesser for Fe₃O₄-water nanofluid.

Appendix A. Supplementary data

Supplementary data associated with this article can be found, in the online version, at <https://doi.org/10.1016/j.rinp.2017.12.026>.

References

- [1] Hiemenz K. Die Grenzschicht an einem in den gleichförmigen Flüssigkeitsstrom eingetauchten geraden Kreiszylinder. *Dinglers Polytech J* 1911;326:321–4.
- [2] Howarth L. The boundary layer in three dimensionless flow-Part II, The flow near a stagnation point. *Philos Mag (Series 7)* 1951;42:1433–40.
- [3] Chiam TC. Stagnation-point flow towards a stretching plate. *J Phys Soc Japan* 1994;63:2443–4.
- [4] Mahapatra TR, Gupta AS. Magnetohydrodynamic stagnation point flow towards a stretching sheet. *Acta Mech* 2001;152:191–6.
- [5] Mahapatra TR, Gupta AS. Heat transfer in stagnation point flow towards a stretching sheet. *H. M. Trans* 2002;38:517–21.
- [6] Nazar R, Amin N, Filip D, Pop I. Stagnation-point flow of a micropolar fluid towards a stretching sheet. *Int J Non-linear Mech* 2004;39:1227–35.
- [7] Reza M, Gupta AS. Steady two-dimensional oblique stagnation point flow towards a stretching surface. *Fluid Dyn Res* 2005;37:334–40.
- [8] Lok YY, Amin N, Pop I. Non-orthogonal stagnation point flow towards a stretching sheet. *Int J Non-linear Mech* 2006;41:622–7.
- [9] Lok YY, Pop I, Ingham DB, Amin N. Mixed convection flow of a micropolar fluid near a non-orthogonal stagnation point on a stretching vertical sheet. *Int J Numer Meth H Fluid Flow* 2009;19:459–83.
- [10] Haq RU, Nadeem S, Khan ZH, Akbar NS. Thermal radiation and slip effects on MHD stagnation point flow of nanofluid over a stretching sheet. *Physica E* 2015;65:17–23.
- [11] Rosali H, Ishak A, Nazar R, Merkin JH, Pop I. The effect of unsteadiness on mixed convection boundary-layer stagnation point flow over a vertical flat surface embedded in a porous medium. *Int J Heat Mass Transfer* 2014;77:147–56.
- [12] Mabood F, Khan WA, Md AI, Ismail, MHD stagnation point flow and heat transfer impinging on stretching sheet with chemical reaction and transpiration. *Chem Eng J* 2015;273:430–7.
- [13] Hsiao K-L. Stagnation electrical MHD nanofluid mixed convection with slip boundary on a stretching sheet. *Appl Ther Eng* 2016;98:850–61.
- [14] Rehman Fiaz Ur, Nadeem S, Haq RU. Heat transfer analysis for three-dimensional stagnation-point flow over an exponentially stretching surface. *Chin J Phys* 2017;55:1552–60.
- [15] Chol SUS. Enhancing thermal conductivity of fluids with nanoparticles. *Off Sci Tech Inf Tech Rep* 1995;231(1):99–105.
- [16] Hamilton RL, Crosser OK. Thermal conductivity of heterogeneous two component systems. *I&EC Fund* 1962;1:182–91.
- [17] Pang C, Lee JW, Kang YT. Review on combined heat and mass transfer characteristics in nanofluids. *Int J Therm Sci* 2015;87:49–67.
- [18] Sarkar J, Ghosh P, Adil A. A review on hybrid nanofluids: recent research, development and applications. *Renew Sustain Energy Rev* 2015;43:164–77.

- [19] Bahiraei M, Hangi M. Flow and heat transfer characteristics of magnetic nanofluids: a review. *J Magn Mater* 2015;374:125–38.
- [20] Bhattacharyya K, Vajravelu K. Stagnation-point flow and heat transfer over an exponentially shrinking sheet. *Commun Nonlinear Sci Numer Simulat* 2012;17:2728–34.
- [21] Bachok Anuar Ishak, Nazar Roslinda, Pop Ioan. Flow and heat transfer at a general three-dimensional stagnation point in a nanofluid. *Physica B: Cond Matter* 2010;405:4914–8.
- [22] Nadeem S, Lee CH. Boundary layer flow of nanofluid over an exponentially stretching surface. *Nanoscale Res. Lett.* 2012;7. article 94.
- [23] Nadeem S, Haq RU, Khan ZH. Heat transfer analysis of water-based nanofluid over an exponentially stretching sheet. *Alexandria Eng J* 2014;53(1):219–24.
- [24] Pal D, Mandal G, Vajravelu K. Flow and heat transfer of nanofluids at a stagnation point flow over a stretching/shrinking surface in a porous medium with thermal radiation. *Appl Math Comput* 2014;238:208–24.
- [25] Hsiao K-L. Nanofluid flow with multimedia physical features for conjugate mixed convection and radiation. *Comput Fluid* 2014;104:1–8.
- [26] Noghrehabadi A, Izadpanahi E, Ghalambaz M. Analyze of fluid flow and heat transfer of nanofluids over a stretching sheet near the extrusion slit. *Comput Fluid* 2014;100:227–36.
- [27] Nadeem S, Hussain ST. Flow and heat transfer analysis of Williamson nanofluid. *Appl Nanosci* 2014;4(8):1005–12.
- [28] Hsiao K-L. Heat transport analysis of unsteady oblique stagnation point flow of elastic-viscous fluid due to sinusoidal wall temperature over an oscillating-stretching surface: A numerical approach. *J Mol Liq* 2016;219:748–55.
- [29] Hsiao K-L. Stagnation Electrical MHD nanofluid mixed convection with slip boundary on a stretching sheet. *Appl T.H. Eng* 2016;98. 850–816.
- [30] Haq RU, Noor NFM, Khan ZH. Numerical simulation of water based magnetite nanoparticles between two parallel disks. *Adv Powder Tech* 2016;27(4):1568–75.
- [31] Hayat T, Nawaz S, Alsaedi A, Rafiq M. Mixed convective peristaltic flow of water based nanofluids with joule heating and convective boundary conditions. *PLoS One* 2016;11(4):e0153537.
- [32] Khan M, Irfan M, Khan WA, Alshomrani AS. A new modeling for 3D Carreau fluid flow considering nonlinear thermal radiation. *Results Phys* 2017;7:2692–704.
- [33] Hayat T, Khan MI, Waqas M, Alsaedi A, Farooq M. Numerical simulation for melting heat transfer and radiation effects in stagnation point flow of carbon-water nanofluid. *Comp Methods Appl Mech Eng* 2017;315:1011–24.
- [34] Rehman Fiaz Ur, Nadeem Sohail. Heat transfer analysis for three-dimensional stagnation-point flow of water-based nanofluid over an exponentially stretching surface. *ASME J Heat Transfer* 2017. <https://doi.org/10.1115/1.4038359>.
- [35] Irfan M, Khan M, Khan WA. Numerical analysis of unsteady 3D flow of Carreau nanofluid with variable thermal conductivity and heat source/sink. *Results Phys* 2017;7:3315–24.
- [36] Khan M, Irfan M, Khan WA. Impact of forced convective radiative heat and mass transfer mechanisms on 3D Carreau nanofluid: A numerical study. *Euro Phys J Plus* 2017. <https://doi.org/10.1140/epjp/i2017-11803-3>.
- [37] Khan WA, Irfan M, Khan M, Alshomrani AS, Alzahrani AK, Alghamdi MS. Impact of chemical processes on magneto nanoparticle for the generalized Burgers fluid. *J Mol Liq* 2017;234:201–8.
- [38] Khan M, Irfan M, Khan WA. Impact of nonlinear thermal radiation and gyrotactic microorganisms on the Magneto-Burgers nanofluid. *Int J Mech Sci* 2017;130:375–82.
- [39] Khan M, Irfan M, Khan WA, Ahmad L. Modeling and simulation for 3D magneto Eyring-Powell nanomaterial subject to nonlinear thermal radiation and convective heating. *Results Phys* 2017;7:1899–906.
- [40] Khan WA, Irfan M, Khan M. An improved heat conduction and mass diffusion models for rotating flow of an Oldroyd-B fluid. *Results Phys* 2017;7:3583–9.
- [41] Khan WA, Khan M, Irfan M, Alshomrani AS. Impact of melting heat transfer and nonlinear radiative heat flux mechanisms for the generalized Burgers fluids. *Results Phys* 2017;7:4025–32.
- [42] Khan M, Irfan M, Khan WA. Numerical assessment of solar energy aspects on 3D magneto-Carreau nanofluid: A revised proposed relation. *Int J Hydrogen Energy* 2017;42:22054–65.
- [43] Sheikholeslami Mohsen, Rokni Houman B. Effect of melting heat transfer on nanofluid flow in the presence of a magnetic field using the Buongiorno Model. *Chin J Phys* 2017;55(4):1115–26.
- [44] Bachok Anuar Ishak, Pop Ioan. Boundary layer stagnation-point flow and heat transfer over an exponentially stretching/shrinking sheet in a nanofluid. *Int J Heat Mass Transfer* 2012;55:8122–8.
- [45] Sheikholeslami M, Rokni HB. Influence of melting surface on MHD nanofluid flow by means of two phase model. *Chin J Phys* 2017;55(4):1352–60.
- [46] Haq RU, Rashid Irfan, Khan ZH. Effects of aligned magnetic field and CNTs in two different base fluids over a moving slip surface. *J Mol Liq* 2017. <https://doi.org/10.1016/j.molliq.2017.08.084>.
- [47] Hayat T, Nadeem S. Heat transfer enhancement with Ag-CuO/water hybrid nanofluid. *Results Phys* 2017;7:2317–24.
- [48] Tiwari RK, Das MK. Heat transfer augmentation in a two-sided lid-driven differentially heated square cavity utilizing nanofluids. *Int J Heat Mass Transfer* 2007;50:2002–18.
- [49] Abu-Nada E. Application of nanofluids for heat transfer enhancement of separated flows encountered in a backward facing step. *Int J Heat Fluid Flow* 2008;29:242.
- [50] Abu-Nada E, Oztop HF. Effects of inclination angle on natural convection in enclosures filled with Cu-water nanofluid. *Int J Heat Fluid Flow* 2009;30:669–78.
- [51] Talebi F, Houshang A, Shahi M. Numerical study of mixed convection flows in a square lid-driven cavity utilizing nanofluid. *Int Commun Heat Mass Transfer* 2010;37(1):79–90.
- [52] Brikman HC. The viscosity of concentrated suspensions and solutions. *J Chem Phys* 1952;20:571–81.
- [53] Xuan Y, Li Q. Investigation on convective heat transfer and flow features of nanofluids. *ASME J Heat Transfer* 2003;125:151–5.
- [54] Li, Q., and Xuan, Y., 2000, "Experimental Investigation on Transport Properties of Nanofluids", *Heat Transfer Science and Technology* 2000, Wang Buxuan, ed., Higher Edu. Press., 757–762.
- [55] Liao SJ. An approximate solution technique not depending on small parameters: a special example. *Int J Non-linear Mech* 1995;30(3):371–80.
- [56] Liao SJ. Homotopy analysis method: a new analytic method for nonlinear problems. *Appl Math Mech* 1998;19(10):957–62.
- [57] Liu CS. The essence of the homotopy analysis method. *Appl Comp* 2010;216:1299–303.
- [58] Liao SJ. Beyond perturbation: introduction to the homotopy analysis method. CRC Press LLC; 2004.
- [59] Oztop HF, Abu-Nada E. Numerical study of natural convection in partially heated rectangular enclosures filled with nanofluids. *Int J Heat Fluid Flow* 2008;29:1326–36.